

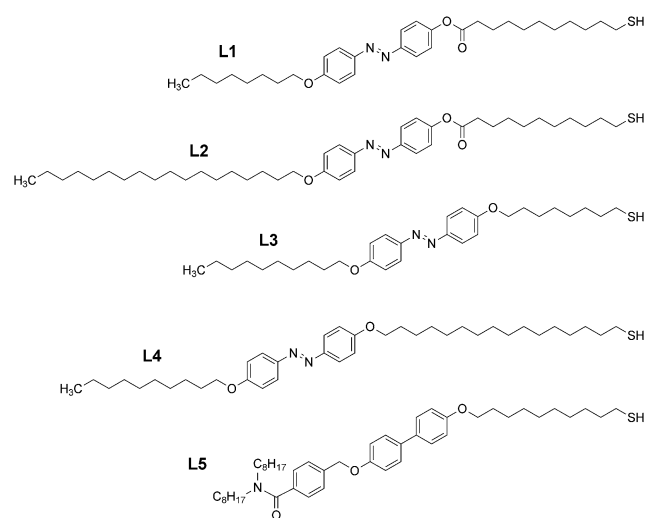
# Phototunable Liquid-Crystalline Phases Made of Nanoparticles\*\*

Anna Zep, Michal M. Wojcik, Wiktor Lewandowski, Kaja Sitkowska, Aleksander Prominski, Jozef Mieczkowski, Damian Pocięcha, and Ewa Gorecka\*

**Abstract:** The properties of liquid-crystalline (LC) hybrid systems made of inorganic nanoparticles grafted with photosensitive azo compounds are presented. For materials with a large density of azo ligands at the surface, the LC structure can be reversibly melted by UV light, and the return to the LC state does not require the absorption of visible light. For systems with a lower density of azo ligands, UV light causes shortening of the distance between metal sublayers in the lamellar phase. Interestingly, the azo derivatives attached to the nanoparticle surface show very different kinetics of *cis/trans* conformational change as compared to the free molecules. The *cis* form of free ligands in solution is stable for days, whereas the isomerization of molecules attached to the nanoparticle surface to the *trans* form takes only a few minutes. Apparently, owing to the crowded environment, azo ligands immobilized at a metal surface behave as they would in the condensed state.

Photoisomerization phenomena open the possibility of the creation of new materials with phototunable properties. Azobenzene derivatives are the most thoroughly studied photochromic molecules. The thermodynamically stable *trans*-azobenzene unit undergoes isomerization to the *cis* conformer upon the absorption of UV light, and *cis*-to-*trans* isomerization can occur thermally or upon the absorption of visible light. Soft materials, such as polymers, elastomers, and liquid crystals, constructed from molecules containing azobenzene moieties have been used in applications such as photomechanical motion,<sup>[1,2]</sup> rewritable holograms or tunable gratings,<sup>[3–5]</sup> and photoinduced alignment.<sup>[4,6,7]</sup> Some examples of photoswitchable hybrid materials made of inorganic nanoparticles (NPs) grafted with azobenzene derivatives were also described.<sup>[8]</sup> UV light triggers the melting of supercrystals of such hybrids into amorphous aggregates. It was shown that this process can be reversed by the absorption of visible light. Since the plasmonic properties of NPs depend on the interaction between metallic cores, the ligand-mediated melting/deformation of NP structures offers an opportunity to tune plasmon resonance by light absorption. In future, light-reconfigurable metallic circuits<sup>[9]</sup> or programmable optical media<sup>[10]</sup> could be obtained.

Herein we present the properties of liquid-crystalline hybrid systems made of inorganic nanoparticles (gold and silver) coated with photosensitive, mesogenic azo compounds. In our studies, we employed a two-step approach for the synthesis of grafted nanoparticles. The spherical gold clusters (**AuC<sub>6</sub>**) were obtained by the slightly modified Brust–Schiffrin method<sup>[11,12]</sup> by using *n*-hexanethiol to passivate the metallic surface. A primary coating of *n*-alkyl thiols improves the solubility of NPs and prevents their aggregation. The size of the metal center, (2.5 ± 0.4) nm, was determined by transmission electron microscopy (TEM) imaging and small-angle X-ray scattering (SAXS) of particles dissolved in toluene. The results were confirmed by analysis of the size-dependent broadening of wide-angle diffraction signals related to the gold crystal lattice. No long-range order was observed for **AuC<sub>6</sub>** NPs, probably owing to their relatively broad size distribution (see the Supporting Information). A previously described method was modified for the preparation of silver nanoparticles covered with *n*-hexanethiol (**AgC<sub>6</sub>**).<sup>[13,14]</sup> TEM and SAXS studies of **AgC<sub>6</sub>** provided a silver-core diameter of 4.2 nm with a distribution of 0.3 nm, and showed a clear tendency of **AgC<sub>6</sub>** NPs to pack into a 2D hexagonal structure (see Figure S7 in the Supporting Information). In the next step, some of the primary grafting thiol molecules were replaced with promesogenic, photochromic molecules by a ligand-exchange reaction.<sup>[15]</sup> Four promesogenic ligands **L1–L4** were used (Scheme 1; see the Supporting Information for their synthesis and spectral characterization). Molecules **L1–L4** have the same mesogenic unit, built of two aromatic rings joined by an azo group



**Scheme 1.** Molecular structures of promesogenic thiols used for grafting on gold and silver metallic clusters.

[\*] A. Zep, Dr. M. M. Wojcik, Dr. W. Lewandowski, K. Sitkowska, A. Prominski, Prof. J. Mieczkowski, Dr. D. Pocięcha, Prof. E. Gorecka  
Department of Chemistry, University of Warsaw  
Al. Zwirki i Wigury 101, 02-089 Warsaw (Poland)  
E-mail: gorecka@chem.uw.edu.pl

[\*\*] This research was financed by the NCN (project 2013/08M/ST5/00781).

Supporting information for this article is available on the WWW under <http://dx.doi.org/10.1002/anie.201407497>.

(azobenzene derivatives), and differ only in the chain length of the substituents on this mesogenic unit and the way in which these terminal chains are connected to the core structure. Covalent bonding of the ligand molecules to the nanoparticle surface was assured by a thiol group at the end of one of the terminal chains. No mesomorphic behavior was observed for these ligands. However, synthetic intermediates with a bromine atom instead of the thiol group formed smectic phases (see the Supporting Information).

To determine the exact composition of organic coronas of the studied nanoparticles, we used various analytical techniques, including thermogravimetric analysis (TGA), TEM,  $^1\text{H}$  NMR spectroscopy, and XPS (see the Supporting Information). According to the results obtained and on the basis of theoretical predictions reported by Murray and co-workers,<sup>[16]</sup> we estimated that on average each gold nanoparticle is covered with 92 ligands and each silver nanoparticle is covered with 410 ligands. The ratio of mesogenic to *n*-alkyl thiols is approximately 1:1 (see the Supporting Information for the composition of organic coronas of the hybrid systems studied).

The liquid-crystalline properties of the hybrid nanoparticles were investigated by XRD and TEM. Homogeneously aligned samples were obtained by shearing a small amount of the material at a slightly elevated temperature (ca. 70 °C) on a Kapton tape. All hybrid materials composed of gold nanoparticles covered with *n*-hexanethiol and promesogenic ligands exhibited long-range positionally ordered structures, of either the lamellar or the columnar type (Table 1).

**Table 1:** Phase sequence of the hybrid nanoparticles.

Compound	Phase sequence
<b>AuL1</b>	Lam 160 °C Iso
<b>AuL2</b>	Lam 160 °C Iso
<b>AuL3</b>	Lam 165 °C Iso
<b>AuL4</b>	Col 155 °C Iso
<b>AuL2L5</b>	Lam 165 °C Iso
<b>AgL1</b>	no LC phase
<b>AgL2</b>	no LC phase
<b>AgL3</b>	no LC phase
<b>AgL4</b>	Lam 157 °C Iso

Lam = lamellar phase, Col = columnar phase, Iso = isotropic liquid.

Gold particles coated with ligands **L1**, **L2**, and **L3** formed lamellar phases, in which layers of metallic clusters were separated by organic layers formed mainly by mesogenic ligands. Their X-ray diffraction patterns showed commensurate, sharp Bragg reflections corresponding to layer periodicity along the direction perpendicular to the shearing, and a weak, diffused signal at the equatorial position owing to the short-range order of particles within the metal-rich layer. The distance corresponding to the diffused signal is similar to the interparticle distance measured for nanoparticles before the ligand-exchange reaction; apparently, promesogenic ligands only weakly contribute to the in-plane separation of nanoparticles. Thus, it can be assumed that the lamellar phase is obtained by redistribution of the secondary grafting molecules around the metallic cluster, the mesogenic cores of

secondary ligands are collected mainly above and below the clusters. For the material **AuL4**, the X-ray diffraction pattern is characteristic of a columnar structure (see Figure S8), which is formed by chains of metal spheres surrounded by mesogenic ligands collected mainly at the equatorial plane of each metal sphere. When heated, the lamellar and columnar phases reversibly melted to the isotropic liquid; in the isotropic phase, a single diffused signal related to the average distance between particles was observed in the X-ray diffraction pattern. The transition between the isotropic liquid and the positionally ordered phases is triggered by changes in the distribution of mesogenic ligands around the metal cluster.

The lamellar phase was also observed for **AuL2L5**, a hybrid material with a low density of photoactive ligands in the organic corona. **AuL2L5** is composed of gold nanoparticles grafted with two promesogenic ligands: the azo derivative **L2** and the biphenyl derivative **L5**, which was described previously as a promesogenic agent that promotes liquid-crystalline polymorphism of gold nanoparticles.<sup>[17]</sup> Silver-based hybrid materials with promesogenic ligands **L1–L3**, which have 8 or 10 methylene groups between the thiol functionality and the mesogenic core, exhibited only short-range order. Apparently, in the case of larger metallic clusters, such a linkage is too short to assure sufficient flexibility of the grafting layer for the formation of an ordered structure. However, when the spacer between the metal surface and the ligand core was extended to 16 methylene groups, as in **AgL4**, the lamellar phase was observed. In contrast to gold-based hybrids, the lamellar phase of **AgL4** showed weak optical birefringence (see Figure S5) as evidence of some degree of orientational order of the mesogenic cores in the organic sublayers.

All mesophases of hybrid nanoparticles were photoresponsive owing to the presence of photoactive azo units in their organic coronas. The liquid-crystalline ordered structures formed by NPs could be reversibly melted by irradiation of the sample with UV light (wavelength 365 nm), which led to the isomerization of azo units from the *trans* to the *cis* conformation. Apparently, ligand isomerization to the kinked *cis* form disturbed the reshaping of hybrid NPs into anisotropic objects as required for their self-assembly into the LC phase. The process could be followed by X-ray diffraction: Under UV irradiation, the XRD signals related to the LC phase of the hybrid NPs disappeared, and a diffused signal corresponding to the average distance between NPs in the isotropic liquid appeared that indicated a slightly smaller distance than in the temperature-induced isotropic phase. The difference can be attributed to the different length of ligand molecules in the *cis* and *trans* conformations. When the UV light was turned off, the LC phase was restored immediately, with layer periodicity the same as before irradiation (Figure 1). No absorption of visible light is even necessary to restore the *trans* conformation of the azo groups; apparently, in the condensed state, the linear, *trans* conformation of ligand molecules is strongly favored over the kinked, *cis* conformation.

For comparison, we also studied the hybrid material **AuL2L5**, in which the density of photoactive units in the secondary grafting layer was lowered by the use of coligands

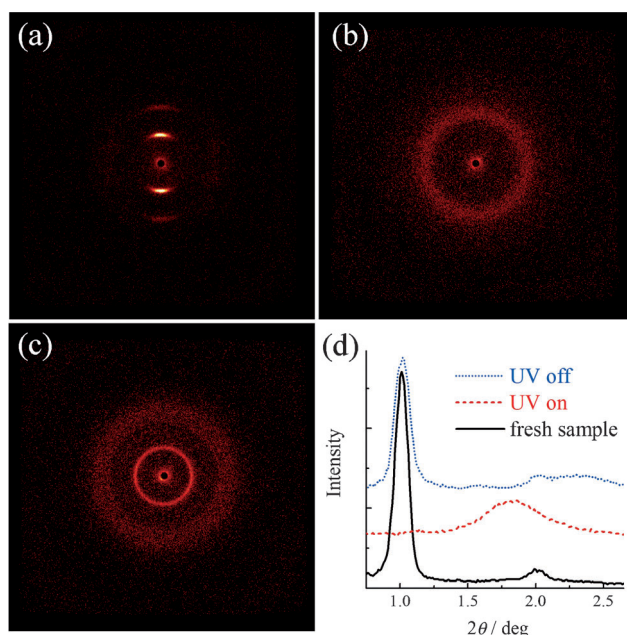


**Figure 1.** XRD patterns obtained for gold NPs **AuL3**. a) Sample oriented by shearing; the sharp reflections correspond to a layer thickness  $d = 78$  Å. b) Sample irradiated with UV light; the diffused signal corresponds to the average distance between NPs (43 Å). c) Sample after switching the UV light off; the lamellar structure has been restored. d) Intensity of XRD signals as obtained by integration of the above patterns over the azimuthal angle.

without azo groups. In this case, instead of melting of the lamellar phase, UV light causes shortening of the distance between metal-rich planes (Figure 2). Such a change in layer thickness should produce instability in the system and thus lead to defects, as observed for smectic phases under sudden stress;<sup>[18]</sup> however, since the lamellar phase of **AuL2L5** is not birefringent, the defects are not easy to observe. The original,

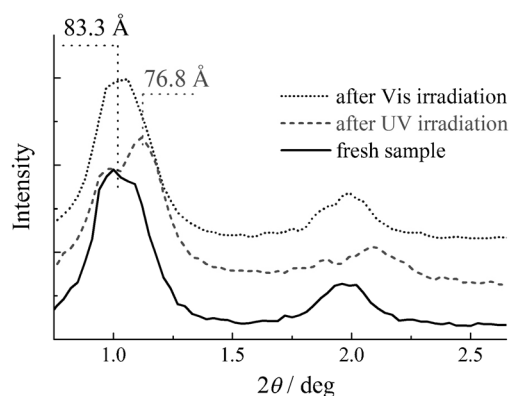


**Figure 2.** XRD diffractograms obtained for **AuL2L5** hybrid NPs functionalized with the azo derivative **L2** and the biphenyl derivative **L5**. Solid line: Fresh sample. The sharp reflections correspond to a layer thickness of  $d = 83.3$  Å. Dashed line: Sample irradiated with UV light. The Bragg signal corresponds to the lower distance between layers of  $d = 76.8$  Å. The presence of the signal for the original layer thickness is due to the large sample thickness, which prevented the bulk absorption of UV light. Dotted line: Sample irradiated with visible light. The lamellar structure with a periodicity of 83.3 Å has been restored.

larger distance between metal-rich planes can be restored by thermal relaxation or through the absorption of visible light.

The *trans*–*cis* photoisomerization of azo units in hybrid materials was also monitored by visible-light absorption spectroscopy and compared to the behavior of free ligands. In solution, all azo derivatives **L1**–**L4** show strong  $\pi$ – $\pi^*$  absorption at 350 nm, as typical for the *trans* form; in the solid state, this absorption is strongly blue-shifted to 300 nm (Figure 3). Hybrid NPs containing azo ligands are in the

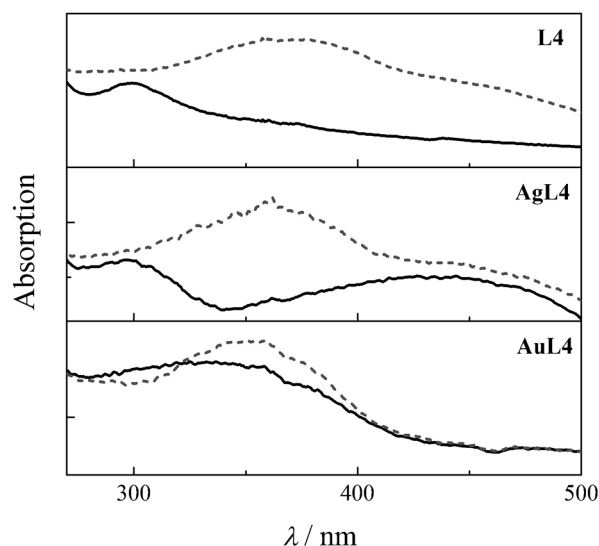


**Figure 3.** UV/Vis spectra for ligand **L4** in the crystal phase at room temperature (solid line) and molten at 100°C (dashed line; top graph); for **AgL4** (hybrid silver nanoparticles covered with ligand **L4**) at room temperature (solid line) and in the lamellar phase (dashed line) at 150°C (middle graph; the absorption band at approximately 450 nm is due to the surface plasmon resonance of silver); and for **AuL4** (hybrid gold nanoparticles covered with ligand **L4**) at room temperature (solid line) and in the lamellar phase at 150°C (dashed line; bottom graph).

condensed state (lamellar or columnar phase) at room temperature, and the position of their  $\pi$ – $\pi^*$  absorption band depends on the type of metal surface: For Au particles, the absorption maximum is at 350 nm, whereas for Ag particles it is at 300 nm (Figure 3). Apparently, at low temperatures, ligands form a nearly crystalline structure in the grafting layer at the silver surface. This solid structure of the ligands in the organic corona of silver-based hybrid particles melts (the  $\pi$ – $\pi^*$  absorption band at 300 nm is replaced by a band at 350 nm; Figure 3, middle graph) at around 150°C, which correlates well with the temperature of structure annealing (sudden increase in the intensity of the X-ray diffraction signals due to the lamellar phase). Apparently, temperature-mediated flexibility of ligand molecules at the metal surface promotes the formation of a long-range lamellar structure.

When hybrid NPs containing azo ligands were dissolved in an organic solvent (chloroform), the  $\pi$ – $\pi^*$  absorption band was observed at 350 nm, as for free molecules. This result shows that the azo ligands remained in the “liquidlike” state, despite being immobilized at the NP surface. However, the

kinetics of the *cis*–*trans* conformational changes of ligand molecules in the grafting layer of the metal particles is very different from that of the free molecules. By monitoring the sample absorption in the visible range, we found that in solution the *cis* form of free azo ligand was stable for hours after the UV light was switched off, as confirmed by the nearly constant intensity of the  $\pi$ – $\pi^*$  absorption at 325 nm that is characteristic of the *cis* form of the azo compound. The absorption of visible light was necessary to induce isomerization back to the *trans* conformation. In contrast, for azo molecules attached to the nanoparticle surface, the *cis* conformation formed upon UV irradiation was strongly unstable, and the *trans* conformation was spontaneously restored within few minutes when the UV light is turned off (Figure 4). Apparently, as a result of the crowded environment, azo ligands at the metal surface show kinetics characteristic for the condensed state.

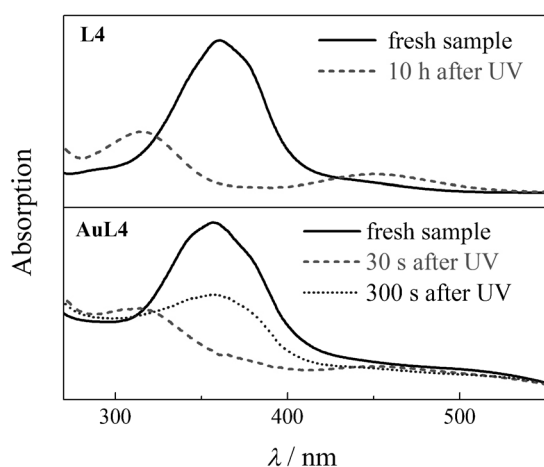


**Figure 4.** UV/Vis spectra for ligand **L4** ( $c = 10^{-6}$  M) dissolved in chloroform before UV irradiation (solid line) and 10 h after the UV light was turned off (dashed line; top graph); and for gold NPs **AuL4** dissolved in chloroform before irradiation (solid line), 30 s after the UV light was turned off (dashed line), and 300 s after the UV light was turned off (dotted line; bottom graph).

In summary, we have obtained phototunable liquid-crystalline structures made of metallic clusters (gold and silver) coated with photosensitive azo molecules. These nanoparticles are the first reported to form either a lamellar or a columnar phase that can be reversibly melted by UV light. In the case of particles with a low density of photosensitive ligands in the organic corona, dynamic control of layer spacing was observed as a result of light-induced conformational changes of the azo ligands in the organic sublayer. The kinetics of the transition is fast, and the

restoration of the original structure does not require irradiation with visible light. These results suggest the design of new LC plasmonic materials with light-controlled optical properties. Such photodriven switching between LC phases could lead to the control of plasmonic properties in future metamaterials, since it offers a feasible way of changing the nearest-neighbor distance between the metallic cores of nanoparticles. This ability to change the distance between nanoparticles in turn translates into tunability of the aggregate permittivity, as has been shown recently.<sup>[19]</sup>

Received: July 22, 2014

Published online: October 8, 2014

**Keywords:** azo compounds · isomerization · liquid crystals · nanoparticles · photosensitive materials

- [1] Y. L. Yu, M. Nakano, T. Ikeda, *Nature* **2003**, *425*, 145–145.
- [2] M. Yamada, M. Kondo, J. Mamiya, Y. Yu, M. Kinoshita, C. J. Barrett, T. Ikeda, *Angew. Chem. Int. Ed.* **2008**, *47*, 4986–4988; *Angew. Chem.* **2008**, *120*, 5064–5066.
- [3] A. Shishido, *Polym. J.* **2010**, *42*, 525–533.
- [4] T. Seki, S. Nagano, *Chem. Lett.* **2008**, *37*, 484–489.
- [5] N. Kawatsuki, T. Hasegawa, H. Ono, T. Tamoto, *Adv. Mater.* **2003**, *15*, 991–994.
- [6] N. Kawatsuki, *Chem. Lett.* **2011**, *40*, 548–554.
- [7] A. Zep, K. Sitkowska, D. Pociecha, E. Gorecka, *J. Mater. Chem. C* **2014**, *2*, 2323–2327.
- [8] R. Klajn, K. J. M. Bishop, B. A. Grzybowski, *Proc. Natl. Acad. Sci. USA* **2007**, *104*, 10305–10309.
- [9] H. Nakanishi, D. A. Walker, K. J. M. Bishop, P. J. Wesson, Y. Yan, S. Soh, S. Swaminathan, B. A. Grzybowski, *Nat. Nanotechnol.* **2011**, *6*, 740–746.
- [10] P. Ahonen, D. J. Schiffrin, J. Paprotny, K. Kontturi, *Phys. Chem. Chem. Phys.* **2007**, *9*, 651–658.
- [11] M. Brust, M. Walker, D. Bethell, D. J. Schiffrin, R. Whyman, *J. Chem. Soc. Chem. Commun.* **1994**, 801–802.
- [12] M. Wojcik, W. Lewandowski, J. Matraszek, J. Mieczkowski, J. Borysiuk, D. Pociecha, E. Gorecka, *Angew. Chem. Int. Ed.* **2009**, *48*, 5167–5169; *Angew. Chem.* **2009**, *121*, 5269–5271.
- [13] Y. Chen, X. Wang, *Mater. Lett.* **2008**, *62*, 2215–2218.
- [14] W. Lewandowski, D. Constantin, K. Walicka, D. Pociecha, J. Mieczkowski, E. Gorecka, *Chem. Commun.* **2013**, *49*, 7845–7847.
- [15] R. S. Ingram, M. J. Hostetler, R. W. Murray, *J. Am. Chem. Soc.* **1997**, *119*, 9175–9178.
- [16] M. J. Hostetler, J. E. Wingate, C. J. Zhong, J. E. Harris, R. W. Vachet, M. R. Clark, J. D. Londono, S. J. Green, J. J. Stokes, G. D. Wignall, G. L. Glish, M. D. Porter, N. D. Evans, R. W. Murray, *Langmuir* **1998**, *14*, 17–30.
- [17] M. M. Wojcik, M. Gora, J. Mieczkowski, J. Romiszewski, E. Gorecka, D. Pociecha, *Soft Matter* **2011**, *7*, 10561–10564.
- [18] N. A. Clark, R. B. Meyer, *Appl. Phys. Lett.* **1973**, *22*, 493.
- [19] K. L. Young, M. B. Ross, M. G. Blaber, M. Rycenga, M. R. Jones, C. Zhang, A. J. Senesi, B. Lee, G. C. Schatz, C. A. Mirkin, *Adv. Mater.* **2014**, *26*, 653.